



Analytical Modeling of Heat Transfer Coefficient Analysis in Dimensionless Number of an Electric Parking Brake Using CFD

V. Agrawal^{*a}, H. P. Khairnar^b

^a Research Scholar of Mechanical Engineering, Veermata Jijabai Technological Institute, Matunga (E), Mumbai, India

^b Faculty of Mechanical Engineering, Veermata Jijabai Technological Institute, Matunga (E), Mumbai, India

PAPER INFO

Paper history:

Received 16 June 2022

Received in revised form 28 July 2022

Accepted 31 July 2022

Keywords:

Brake Mass

Heat Dissipation

Nusselt Number

Clamp Pressure

Emmissivity

ABSTRACT

The present study intends the development of an electric parking brake (EPB) for commercial vehicles (CVs). CVs with EPB applications are currently available in an entirely different set of issues than EPB applications on passenger cars, which are presently widely used. Safe parking requires much more focus with an order of magnitude, more thermal capacity, brake mass, and clamp pressures. In the first instance, heat loss from the brake disc was estimated. The investigations also allowed for precise prediction of radiative heat loss by defining surface emissivity. The parameters of air movement, convective heat transfer coefficients, and velocities were investigated, and validation was done with the CFD model. When the temperature dropped to 252 °C, the maximum estimated value of the Nusselt number was 72.25. Nusselt number pattern that looks identical over the arc surface yields 13.38 percent better results. Nu values at maximum temperature were calculated to be 80.5 and 82.6 at 251.8 °C. The “ h_{conv} ” value was 4.1 percent lower than in the arc region, with the highest value at 400°C being 11.5 W/m²K. The present study adopted unique approach and obtained brake disc temperature and the coefficient of convective heat transfer on disc friction surfaces and hat regions. CFD modeling was done during the cooling phase to evaluate flow patterns and “ h_{conv} ” fluctuation across the entire disc brake surface area. The mathematical modeling and adopted methodology for computing heat transfer coefficients for different disc regions have helped to better understand of a CV brake disc heat dissipation.

doi: 10.5829/ije.2023.36.02b.08

NOMENCLATURE

CFD	Computational fluid dynamics	Nu	Nusselt number
CV	Commercial vehicle	Pr	Prandtl number
EPB	Electric parking brake	Ra	Rayleigh number
HTC	Heat transfer coefficient	Re	Reynolds number
FE	Finite Element	T	Temperature
OD	Outer diameter	v	Velocity
C_p	Specific heat capacity	r	Radius
A	Surface area	Greek Symbols	
D	Disc diameter	ρ	Density (kg/m ³)
y_r	Wall characteristic length	μ	Dynamic viscosity (kg/ms ²)
Gr	Grashof number	ν	Kinematic viscosity (m ² /s)
h	Heat transfer coefficient	t	time (s)
k	Thermal conductivity	ν	Kinematic viscosity (m ² /s)
l	Length	L	Characteristic length (m)
m	Mass	Subscripts	
p	Pressure	α	Thermal diffusivity
Q	Cooling power	ϵ	Emmissivity
Q	Cooling power	ϵ	Emmissivity

*Corresponding Author Institutional Email: vkagrawal_p18@me.vjti.ac.in
(V. Agrawal)

Please cite this article as: V. Agrawal, H. P. Khairnar, Analytical Modeling of Heat Transfer Coefficient Analysis in Dimensionless Number of an Electric Parking Brake Using CFD, *International Journal of Engineering, Transactions B: Applications*, Vol. 36, No. 02, (2023), 276-288

1. INTRODUCTION

The objective is to contribute to the development of commercial vehicle (CV) electric parking brakes (EPB). Despite being widely used in passenger cars today, EPB applications on CVs present entirely different challenges. In the research process, typical dimensionless air properties were used to investigate over a simplified brake disc friction surface, deviation in mean local convective heat transfer coefficients. For the entire cooling process, a nonlinear equation was used to calculate the average convective heat transfer coefficient at the surface fluctuation when it comes to temperature reduction. First-order differential equations were built based on fundamental principles of bulk disc temperature. A good correlation with observed values was attained, to within 10%, by including variations during the cooling period. Heat is dissipated through convection and radiation. Until now, there has not been much research on geometric shape heat dissipation from a stationary disc. In the same way, there is not a lot of research on the cooling of stationary brake discs. Due to the task's relative design robustness, this was formerly assumed to be a technical issue that received little attention. The electrification of braking systems, as well as recent breakthrough in automotive development, however, is necessary to gain a better understanding of thermal brake characteristics in stationary settings. This knowledge will undoubtedly aid in predicting temperature in a variety of driving situations. Brake temperatures at the disc interface have a significant impact based on friction coefficient and pad wear. It has been explored chiefly for moving vehicles in the past. For city buses, stationary brake cooling is very crucial, and they spend a significant amount of time waiting at bus stops, traffic lights, and other such sites.

It was discovered that the stationary disc brake had the highest coefficient of heat transfer. It is obvious that the presence of disc has increased the air flow and turbulence in the rotor, resulting in a higher value of coefficient of heat transfer. A rise in thermal conductivity with temperature prevents the appearance of the apex h_{conv} value, as it does the Nusselt number. It was observed that the value of h_{conv} was higher along with the value of maximum heat transfer coefficient.

Figure 1 depicts the research methodology adopted in heat transfer analysis of the stationary disc brake. In the analytical-numerical modeling is the topic of research on the heat dissipation using conduction, convection and radiation of the discs over an extended period. Investigates the brake disc of outboard and inboard view of the disc brake, and computed the temperature and convective heat transfer coefficients based on CFD modeling.

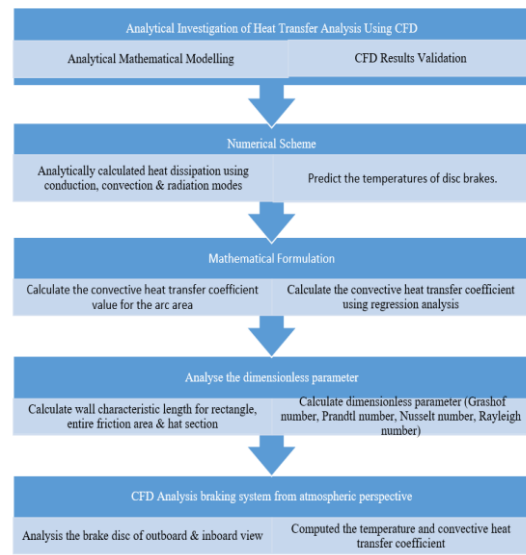


Figure 1. Research methodology adopted in heat dissipation

2. LITERATURE REVIEW

Most current EPB research publications focus on the EPB's motor control system. For example, sensorless position and velocity monitoring enable more precise EPB actuation control [1]. However, the motor response time of a fuzzy-type numerical controller is faster than that of typical PID controllers [2]. If any frequent EPB errors occur, to transmit driver notifications, a technique for detecting faults has been developed [3]. Therefore, friction coupling cooling is integral to any braking system's thermal concerns.

Many vane arrangements have been used in convective cooling by optimizing air movement across the disc [4]. Because the air is driven through the vanes at a greater rate as the vehicle speed increases, convection significantly affects brake cooling. The flow of air quality is equally as crucial as the speed with which it moves. The vanes produce recirculation zones, which diminish the convection process [5]. Brake designers and academics have turned to CFD modeling procedures to understand better the convective heat transfer coefficients and the resulting flow field. Flow separation straight vane rotors have a leading-edge surface that has been effectively demonstrated using CFD. Resulting in a lower convective heat transfer coefficient [6]; the leading edge, in contrast to the trailing edge, a steady air flow can be seen down the vane.

Brake temperature levels can be reliably predicted subject to properly stated boundary conditions using finite element (FE) methods [7]. Both disc temperatures were computed using a linked thermo-mechanical FE

model, and thermal strains induced in the event of a complex braking situation further demonstrated the utility of FE analysis and enabled researchers to predict the occurrence of thermal cracks in the rotors [8]. Nusselt number pattern looks identical over the arc surface using his correlation equation [9, 10].

The vertical friction surfaces provide the majority of convective cooling because the rotor section's thickness is significantly less than the OD [11]. The correlation approach provides values that are closer to experimental data. Several relationships have been found within the confines of a buoyant fluid flowing across a solid surface [12-22].

The non-Fourier heat conduction in a semi-infinite body was examined. The heat wave non-Fourier heat conduction model was used for thermal analysis. Thermal conductivity was assumed temperature-dependent, which resulted in a nonlinear equation [23]. The temperature gradient and thermal conductivity compute the heat flux through the interface. The uncertainty in the heat flux computation may be examined by comparing the differences in the calculated values of heat flux for both the hot and cold specimens in the steady-state condition [24]. The aero-thermal environment of a TSTO flying test bed has been assessed both from the engineering-based and CFD-based approaches. Computations with the air modeled as perfect gas highlight that vehicle aero heating is more severe than existing reentry vehicles [25].

The approximation order of the optimal control issue for the spatial process of heat conduction. An algorithm for solving the difference problem is explained, and an estimate of the value of the difference functional divergence from the continuous functional is obtained using the methods of integral inequalities and the method of difference approximation [26]. All heavy metals found, with the exception of Fe, (Zn, Ni, Cu, Cr, and Pb), have a close relationship with road traffic, according to the level of heavy metal contamination of roadside soils exposed to road traffic on a major road and the results attained [27, 28].

The research issues currently being explored are summarized in work discussed above. They were all done in dynamic conditions, primarily on passenger automobiles. However, there has been relatively little research on static brake qualities published. Thermal considerations, on the other hand, are critical in hot parking scenarios. The lack of vehicle motion causes only airflow-natural convection results in a significant reduction in cooling rate and a substantial shift in heat flow patterns. Thermal contraction requires more investigation into the impacts of heat transmission by conduction, convection, and radiation.

Because of their reduced size and lower load requirements, they are more popular; passenger vehicle EPBs offer the advantage of over-clamp the brake

without causing damage to the brake caliper fatigue life to mitigate the brake disc and pad thermal contraction effects. Three minutes after the original application, a passenger vehicle EPB re-energizes the brake by applying a second-stage clamp force. On the other hand, CV brakes offer a substantially higher clamp force and thermal capacity, allowing for much more thermal expansion. Longer cooling durations are expected, with increased thermal capacity during the parked brake cooling period. However, higher development induces increased contraction, resulting in brake performance uncertainty. As a result, EPBs have not yet been fully integrated into CVs. The introduction of EPB to CVs spurred this research into several aspects and influencing parameters on static disc cooling. The ultimate goal is to create reliable and accurate prediction models that shorten the time to market.

3. MATHEMATICAL MODEL

It has been shown to be more challenging to model stationary disc brakes heat transfer than to model heat transfer in dynamic situations. Short braking periods and disc rotation, symmetry around constant heat transfer coefficients for constant heat transfer coefficients (HTC) for each vane channel are reasonable assumptions. Because natural convection is the only source of airflow, cooling times are substantially longer in stationary parking conditions. Coefficients of heat transmission can no longer be thought of as constant. The disc brake's convective heat transmission variability must be understood to provide an accurate temperature forecast technique. All the modelings were done with the brake disc shown in Figure 1, and the purpose of testing was to obtain this knowledge. The disc is constructed of grey cast iron and features a straight vane vented shape that prevents it from coming (Figure 2).

Table 1 provides more information about the braking disc used. The disc has an anti-coning shape, meaning the friction face on the inboard side is not concave. As the word implies, there is no considerable coning due to the thermal expansion, specifically, a difference in axial



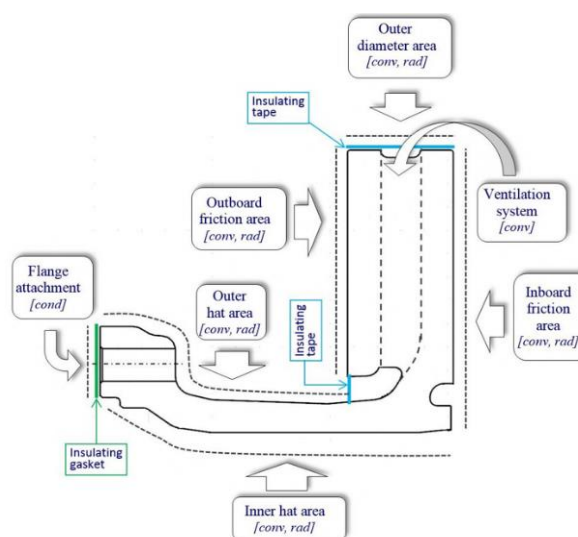
Figure 2. Brake disc analysed: a) Outboard view; b) Inboard view

TABLE 1. Characteristics of disc brake

Specification	Dimension
Outside friction diameter (mm)	434
Inside friction diameter (mm)	234
Thickness of the rotor (mm)	45
Weight (N)	380
Number of vanes	30

displacement between the outer and inner diameter of the disc. Since friction surfaces are kept level, this disc type has a lower risk of brake judder caused by uneven pad wear. The air enters through the side that faces outward, passing through a small gap between the inner diameters of the hub and disc before turning 90 degrees and flowing radially via the channels towards the disc's outer diameter. Furthermore, this disc is subjected to more significant thermal stresses in the disc transition zone than the standard disc design. The disc features 30 straight radial vanes and an overall thickness of 45 mm, channel width with two 14 mm thick walls separated by a 17 mm gap.

The brake disc was heated consistently to a higher temperature in all of the analyses in this study. Figure 3 and Table 2 show the heat dissipation zones and their associated modes. The disc ventilation system was shut down by using temperature-resistant tape to block the channel entry and exit points (Figure 2). Reduce noise; an insulating gasket was installed between the disc hat and the wheel carrier flange to analyze efficiently, and precisely all modes of heat transport have been investigated and adequately modeled.

**Figure 3.** Areas of the discs and the heat dissipation modes [21]**TABLE 2.** Modes of heat dissipation and their associated locations

Total convective area (m ²) = 0.658					
Total conductive area (m ²) =0.025	Outer hat	Friction outboard	Friction inboard	Outside diameter	Ventilation system
	0.104	0.105	0.119	0.0166	0.313
Total radiative area (m ²) = 0.35					

4. ANALYTICAL INVESTIGATION

Conduction transports heat from the wheel carrier to the disc through the contact zone, as depicted in Figure 3: Flange attachment. In the vehicle installation, 10 M16 bolts with a torque of 330 N-m are used for fastening. Heat can move in either direction, but because the disc is usually at a greater temperature, the conductive transfer is primarily from the disc to the wheel carrier. Thermal contact resistance will inevitably exist due to imperfections in the surfaces in contact, inhibiting heat transmission and producing temperature differences between the interfaces.

In practice, the thermal conductance parameter, as many writers employ, is the best way to explain this phenomenon. Heat is transported through conduction according to Equation (1).

$$Q = h_{\text{cond}} A_{\text{cond}} (T_d - T_c) \quad (1)$$

The conditions of interface surfaces, the material employed, and the force clamp used to determine thermal conductance. If the conductance, interface temperature, and contact area differential are all high, the heat transfer rate will be faster. Tirovic and Voller [9] devised an experiment to determine heat conductivity for this sort of material (spheroidal cast iron wheel carriage and grey cast iron disc), surface coatings, and the state of the contact surface. Since the pressure at the interface determines conductance, these values will vary depending on which side of the interface, Equation (2) average values in engineering calculations for bulk heat transfer:

$$h_{\text{conv}} = 800P_{\text{avg}} + 2300 \quad (2)$$

The previous calculation yields h_{cond} (avg) in [W/m² K]. Calculate the average interface pressure and total clamping force (due to 10 bolts) divided by the region of the user interface. The bolt tightening torque can be used to estimate clamp force. Heat transmission to and during protracted cooling periods, the temperature of the wheel carrier may fluctuate, and conduction will be challenging to incorporate into simplified models. This effect is unlikely to be significant when considering small conductive elements due to the short contact area. As a result, it was determined that at this time, it would be

preferable to use a thermal insulating gasket at the disc interface to reduce bolt clamping force.

In most braking circumstances, convection is the primary heat transfer method, and it is highly dependent on vehicle speed. Therefore, it requires special attention. The minimum feasible convective heat transfer that will be used in the rotating disc speed is zero in the case under investigation. Furthermore, in driving situations, the disc's temperature has a minor effect on the convective heat transfer coefficient. Because the surface is given fresh air, when the temperature rises, only a slight decrease in the convective heat transfer coefficient occurs. Only natural convection occurs in stationary conditions. Therefore, the scenario is fundamentally different. The temperature difference between the disc-air is the only driving force, and the hotter, more excellent disc is the h_{conv} , resulting in the total heat released. Convective cooling power is identical to conductive cooling power in Equation (3).

$$Q_{conv} = h_{conv}A_{conv}(T_d - T_a) \quad (3)$$

Convective heat transfer coefficient values will differ throughout disc areas, and T_d temperatures will almost certainly differ over broad disc surfaces. As a result, convective cooling becomes much more difficult, and the required 'averaging' is more susceptible to assumptions, simplifications, and mistakes. The disc ventilation system's heat transport (channels and vanes), as well as air temperatures near the disc and coefficients of local convective heat transfer will be studied in Part 2 of this paper using CFD modelling. The first stage is focused towards achieving this. The ventilation system was turned off at the channel entry (inside disc diameter) and exit for this preliminary stage of analysis (outside disc diameter). Although radiant heat dissipation is usually associated with extreme heat and is often overlooked, In the case of a fixed disc, since convective cooling is minimal. Radiative heat dissipation's basic formula in Equation (4).

$$Q_{rad} = (T_d^4 - T_a^4) \quad (4)$$

An average emissivity value of 0.92 was found in the investigation of this research and will be used as a parameter in the simulation of this specific disc under test conditions. Because the ventilation system has no radiative heat loss to the environment, the disc area emitting heat via radiation is substantially lower than the convective area. Boundary conditions become significantly more difficult when the brake is mounted within the wheel cavity due to radiative transmission. The conductive and convective modes can be represented in Equation (5).

$$Q_{rad} = h(T_d - T_a) \quad (5)$$

The coefficient of convective heat transfer on disc friction surfaces and hat regions was determined using

analytical methods. Numerical models were then used to predict the temperatures of disc brakes. The investigations also allowed for precise prediction of radiative heat loss by defining surface emissivity. Finally, temperatures were measured and calculated, and the results were compared.

Since there has been no previous work on analytical modeling of the geometry of a CV brake disc, no precedent for establishing accurate temperature forecasts has been established. A series of local h_{conv} values were created using a reduced brake disc design, which was then averaged throughout the entire friction surface. As illustrated in Figure 4, dimensionless parameters were derived using well-known literature equations, and friction surface geometry partitions were then projected as sections of the simplified friction surface geometry. After averaging these values throughout the total surface area, for the temperature range pertinent to CV parking applications, an equation for average h_{conv} was derived. Finally, the hat region was subjected to the same analytical procedure; the concept of horizontal cylinder heat dissipation was employed instead of the vertical wall theory. The cylindrical area at disc OD can be handled in the same way, but it can be ignored because it is insulated and much smaller. The process is easier to understand, and all cooling is supposed to proceed with only a tiny amount of energy delivered to the wheel carrier by conduction. The wheel carrier is heated by convection and radiation. The cylindrical area at disc OD can be handled similarly, but it can be ignored because it is insulated and much smaller. The analytical results will be compared to observed values during validation.

Heavy braking applications can cause brake disc temperatures to exceed 500°C, though it's unlikely that a CV would be parked as a result of an application, reaching and exceeding 400°C regularly. As a result, a parking simulation was planned to start with a 400°C disc brake surface temperature.

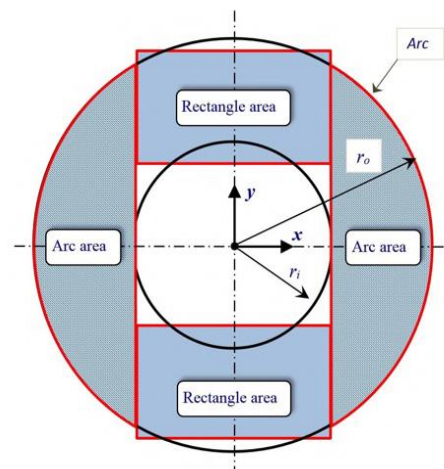


Figure 4. Disc friction surfaces are divided into simpler geometric portions

Natural convection transmission of heat research has been done on bodies of basic geometry throughout history. McAdams [10] showed how a vertically and horizontally positioned flat plate in open-air might produce thermal and hydrodynamic boundary layers. In cylindrical geometry, Morgan [11] demonstrated the same. The vertical friction surfaces provide the majority of convective cooling because the rotor section's thickness is significantly less than the OD. As a result, two vertical plates can be used to approximate the disc in free air. It would be difficult to justify just using McAdams [10] and Churchill and Chu [12] traditional formulae because they were calculated using rectangular plates with constant characteristic lengths in open air. Flow across a known characteristic length local vertical surface is believed to be independent of flow horizontally adjacent to it, and Gr values are calculated accordingly. The air parallel to the surface is unlikely to be affected by the turbulent flow's eddy currents toward the turbulent region lateral flow motion, which will impact parts of the laminar flow areas as they approach the laminar r_0 . Because the mathematical calculations have become more complicated and because of the project's time constraints, this effect cannot be examined further without CFD. For the time being, any turbulence flow will be found on the disc brake surface and be restricted to a direction perpendicular to the horizontal. When examining a single point along the horizontal center line, the size of the Grashof number increases as temperature falls, peaking at 255.6°C. When there is not a temperature gradient, the Grashof number decreases until it reaches zero at room temperature. The temperature change is directly proportional to the Grashof number; the occurrence of the peak Grashof number value is linked to a change in kinematic viscosity. The thermal expansion causes a fluid's density to decrease as its temperature rises. Lowering the kinematic viscosity of a fluid with a lower density reduces during a frictional flow. The viscosity kinematic effects exceed thermal gradient at a temperature of 255.6°C or higher, lowering the Gr value.

The Rayleigh number, Grashof, and Prandtl numbers are multiplied to get the result. Regarding heat transmission from a body in a buoyancy-driven flow, Equation (6) is used instead of the Grashof number. It expresses the proportion of conductive to convective heat transfer. Conduction is the primary heat transport method below the critical temperature, which switches to convection. Ra's critical value varies based on the surroundings and geometry of solid surfaces. An essential factor in a horizontal flat plate, according to McAdams [10], is as low as 10^7 ; in open air, the critical value for vertically stacked cylinders is as high as 10^9 , according to Necati Ozisik [13].

$$Ra = Pr * Gr \quad (6)$$

They consider that Rayleigh number is a Grashof number function. However, the fact that the observed findings are similar is not surprising. McAdams [10] states that at 400°C, turbulent flow is represented by a value of 3.5×10^8 . The results reveal that the airflow only 8 mm from the OD gets turbulent. Necati Ozisik [13] proposed a crucial Ra value for a different shape, indicating that the flow parallel to the arc surface is laminar throughout. Neither of the calculated values was for a character with the same geometry as the arc. Numerical calculations cannot determine whether or not the flow is entirely in a turbulent state. The heat dissipation conclusion cannot be drawn with precision due to the ambiguity of the airflow state. Research suggests that when the disc is at its hottest, the flow will have crossed the boundary between the laminar and turbulent flow.

The fluid characteristics for flow across an arc surface have recently been discovered; the Nusselt number was calculated to better explain the flow will have crossed the boundary between the laminar and turbulent flow. Since the numbers in Equation (6) are not always known, it is not always as straightforward as in the Nusselt number. Small changes in shape have an impact on the buoyant flow's intensity and subsequent parameter values. When it comes to the Nusselt number, it's common to employ approximation formulae derived from analytical data and correlation analysis. Compared to theoretically calculated equations, Necati Ozisik [13] showed that the correlation approach provides values closer to experimental data. Several relationships have been found within the confines of a buoyant fluid flowing across a solid surface. Churchill and Chu [12] proposed a vertical wall correlation equation, when isothermal wall conditions are considered, Rayleigh numbers between 10^{-1} and 10^{12} are valid.

$$Nu = \frac{h_{conv}L}{k} \quad (7)$$

As a ratio of convection to conduction, the Nusselt number indicates energy transfer from the solid surface boundary to the flowing fluid and across its thickness in a normal to the surface direction. Prandtl number, on the other hand, focuses on the moving fluid and the interaction between it and heat dissipation. Nusselt values of unity indicate that heat dissipation from the surface is evenly distributed between conduction and convection, as seen in laminar flow. Convection is dominant in a turbulent flow, Nu will surpass 100 [13]. It is vital to note that the characteristic length of the body's surface is represented by Equation (7). Over the arc region, the Nusselt number will be determined to assist explain the primary mechanism of heat conduction. To determine the mean local Nusselt number, McAdams [10], Equation (8) and Churchill and Chu [12], Equation (9), offered two distinct correlation equations; both were employed and compared, as illustrated in Figure 5. The

mean local Nusselt number from the disc are included in the CFD data. It includes analyses carried out at four temperatures. The effect of temperature of disc and Nusselt number will be determined to assist explain the primary mechanism of heat conduction can thus be studied and analysed in Figure 5.

$$Nu_m^{1/2} = 0.825 + \frac{0.387 Ra_L^{1/6}}{[1 + (0.492/Pr)^{9/16}]^{8/27}} \tag{8}$$

According to Necati Ozisik [13], Equation (9) provided by McAdams [10] better matches results. The final Equation (9) is as follows.

$$Nu_m = cRa_L^n \tag{9}$$

where c denotes a constant and Ra represents Rayleigh number, Table 3 shows these parameter values, which all rely on Ra.

Both ways of computing the Nusselt number generated over the thermal boundary layer mean Nusselt number values. The Churchill and Chu [12] technique was evaluated first, followed by a comparison of the two methods. Nusselt values above 100 denote a convection-dominated surface-to-fluid regime; values one and lower represent through the fluid and away from the surface, and conduction occurs. A value of 71 is predicted by the Churchill and Chu [12] Equation (9), as seen in Figure 4. This value falls in the middle of both crucial values, implying a state of transition in line with previous trends.

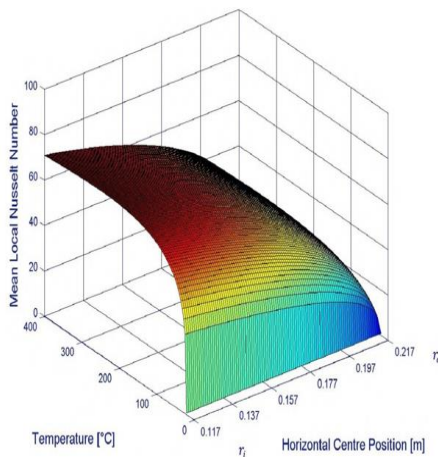


Figure 5. Temperature and horizontal position mean Nusselt number

TABLE 3. Mean Nusselt number parameters for McAdams [10]

Type of flow	Ra value	c	n
Laminar flow	10 ⁴ to 10 ⁹	0.6	0.25
Turbulent flow	10 ⁹ to 10 ¹³	0.11	0.667

The value remains high; while conduction still plays a part, the majority of the heat generated by the arc is dissipated through convection. The maximum estimated value was 72.25 when the temperature fell to 252 °C. The inner radius with the most extended characteristic length was discovered. The Nusselt number is affected by temperature and location as this nonlinear distinct declines. McAdams [10] produced a Nusselt number pattern that looks identical over the arc surface using his correlation equation (as seen in Churchill and Chu's [12] Figure 5. The McAdams [10] equation yields 14 percent better results, Nu values at maximum temperature were calculated to be 80.5 °C and 82.6 °C at 251.8 °C. The heat transmission from the arc surface isn't entirely conventional, even with a significant rise in Nu. The McAdams [10] Equation (9), according to Necati Ozisik [13], is a more accurate representation of the actual value; as a result, all subsequent vertical wall heat transfer calculations will be based on it.

Convective heat transfer coefficient can be calculated after determining that convection transports most heat from the arc surface to the surrounding air. Any h_{conv} estimate must account for the effect of conduction from the surface to the atmosphere. Figure 6 shows the locally computed mean h_{conv} values derived from Equation (5) at various positions around the disc arc area. The convective heat transfer coefficient values vary, ranging from zero to 14.4 W/m² K at the highest temperature. In the region for reference, the appearance of apex h_{conv} value, similarly to the Nusselt number, is prevented by a rise in thermal conductivity with temperature. The magnitude drop as characteristic length decreases towards the outer disc radius exhibits a similar pattern. This is an expected outcome since the thermal boundary layer's typical length shortens, reducing heat transfer. Equation (10) linking convective HTC to temperature and location might be created. Because the goal was to create a total surface relationship for a convective HTC, it was unnecessary to build such a complicated Equation (10). To determine a single average h_{conv} value for the entire arc area, Equation (10) was employed.

$$h_{conv} = \frac{\sum_{i=r_1}^{r_o} h_{conv_i} A_{arc_i}}{k_{arc}} \tag{10}$$

In Figure 5, Equation (10) outcomes regarding the temperature, h_{conv} decreases nonlinearly with cooling. The results were put through a regression analysis to see if there was a link between h_{conv} and temperature. The best estimate was found to be a natural logarithm adjustment term in a quadratic relationship, which caught roughly 98 percent of the data in Equation (11).

$$h_{conv} = a_1 + a_2 T_d + a_3 T_d^2 + a_4 \ln(T_d) \tag{11}$$

The natural logarithm term was used to account for the drop in temperature as it approached ambient. When higher-order terms were added to Equation (11), a

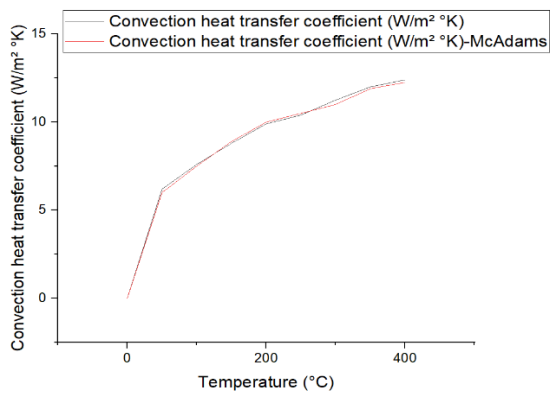


Figure 6. Mean convective heat transfer coefficient values across the arc area for various temperatures

regression equation that described almost 99 percent of the data was obtained, but the improved accuracy was deemed not justifiable due to the additional computational time required. For the arc section, coefficients for Equation (10) have been obtained and are listed in Table 4. The sole limitation to utilizing this Equation (11) is that it does not exactly pass through zero at ambient temperature. As a result, the user must explicitly provide ambient temperature has a h_{conv} value of zero and then let Equation (11) estimate the remainder.

Figure 7 depicts the flow chart analysis of the heat dissipation of the stationary disc brake. The first part of the analytical-numerical modeling is the topic of research on the expected temperatures of the discs over an extended period. In second part investigates air movement, convective heat transfer coefficients, and velocities, validations based on CFD modeling.

5. RESULTS AND DISCUSSION

It was uncertain how much convective heat transfer occurred between the two rectangular zones on the reduced disc brake friction surface shape. Regarding the arc areas, " h_{conv} " equation for a friction surface on a disc brake might be obtained using a similar technique. The capacity to take on a rectangular form has the advantage of allowing the boundary layer on the surface is expected to develop equally in the horizontal direction throughout the entire surface. Results have been discussed considering convective heat transfer in a rectangle, convection transfer of heat during friction as the whole

TABLE 4. Coefficients for the arc area according to Equation (11)

a_1	a_2	a_3	a_4
-10.65	-0.025	3.4×10^{-5}	4.55

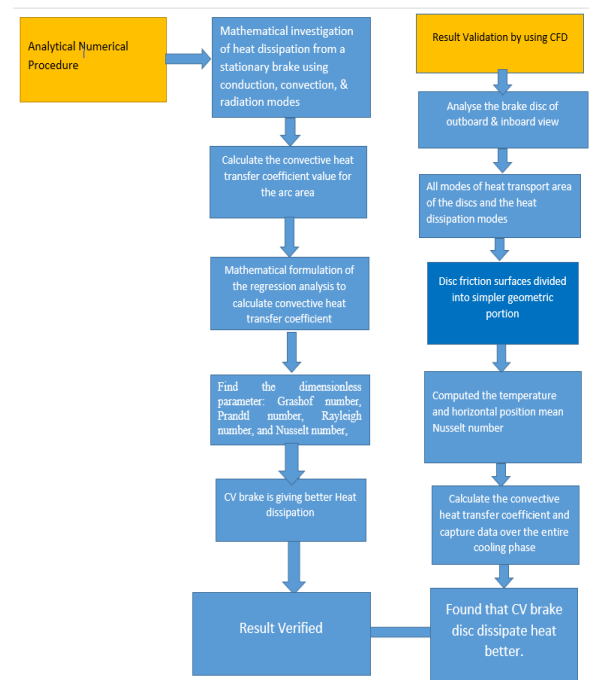


Figure 7. Flow chart for computation of heat transfer of the stationary disc brake

area of the disc, and convective heat transfer over the hat section.

5. 1. Convective Heat Transfer in a Rectangle

As a result, the airflow and heat transmission properties would be uniform across segments, significantly simplifying the operation. As per the design, the rectangle's base lengths equal twice the inner radius dimension. By equating the disc surface area to the four sectors and then adjusting for yr, the height of the rectangle could be calculated analytically. As a result, the size of the reduced geometry was the same as that of the conventional geometry, making them equivalent. The rectangle height was calculated using Equation (12), determined to be 114 mm.

$$y_r = \frac{\pi(r_0^2 - r_i^2)}{4} - 2A_{rec} \quad (12)$$

The characteristic wall length and dimensionless quantities for the rectangle were determined. The temperature range that will be investigated may remain constant. The temperature range under investigation will be consistent, ranging from 20°C to 400°C, and will have equivalent temperature-dependent air characteristics. Figure 9 shows the change in Grashof, Prandtl, Rayleigh, and Nusselt numbers as a function of temperature. Because air is still fluid, Prandtl values decrease as temperature rises; the values are identical to those in the arc region. The Rayleigh, Grashof, and Nusselt numbers

all began at zero and grew nonlinearly to a peak value before vanishing; For the three different dimensionless numbers, 1.15×10^7 , 1.685×10^7 , and 34.6 were the peak values, respectively. The convective HTC result for the rectangle region (shown in Figure 9) displays a pattern similar to the arc area since the same equations and fluid parameters were used (shown in Figures 8-11).

The h_{conv} value was 4.1 percent lower than the arc region; at 400°C, the most significant value was 11.5 W/m² K. Table 5 shows the coefficients for Equation (11) to create a regression equation for predicting h_{conv} values.

5. 2. Convection Transfer of Heat Over the Entire Friction Area of the Disc

Since the brake disc geometries was simplified, two independent investigations of the disc friction surface and heat transmission zones could be developed. The result is a weighted average comparable measurement that was used to obtain a broad comprehension of the whole disc brake surface's heat transmission variation as a function of temperature. The arc surface area accounts for half of the surface total contact face area, giving it a weight

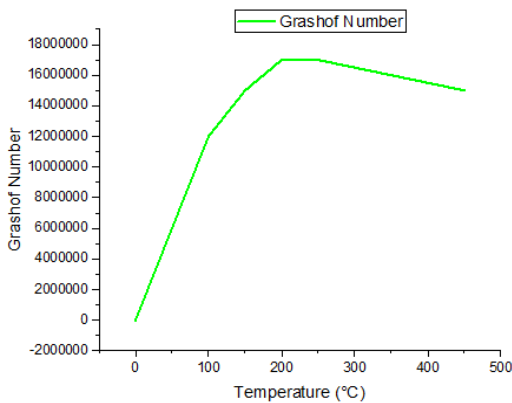


Figure 8. Grashof number vs temperature for the rectangular area

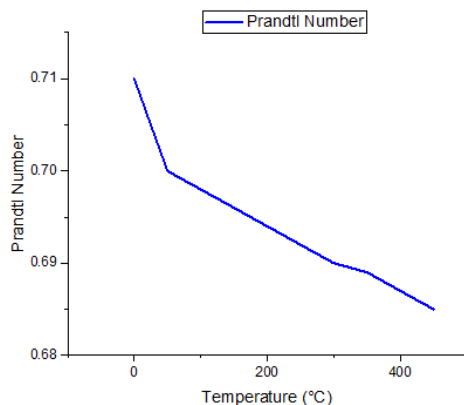


Figure 9. Prandtl number vs temperature for the rectangular area

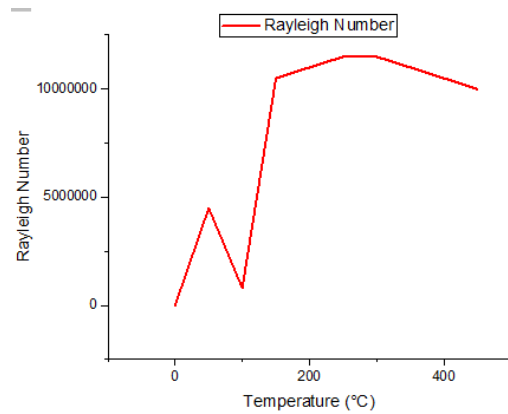


Figure 10. Rayleigh number vs temperature for the rectangular area

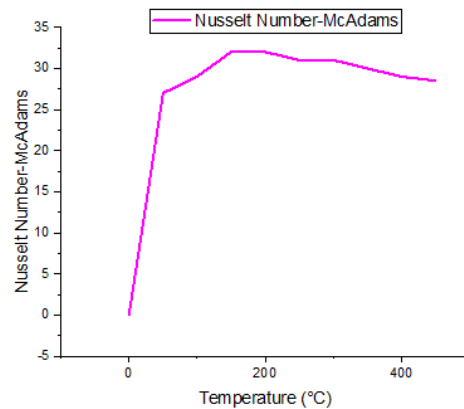


Figure 11. Nusselt number vs temperature for the rectangular area

TABLE 5. Coefficients for the rectangle area according to Equation (11)

a_1	a_2	a_3	a_4
-10.225	-0.0245	3.3×10^{-7}	4.35

TABLE 6. Coefficients equivalent Equation (11) to friction area

a_1	a_2	a_3	a_4
-8.08	-0.019	2.55×10^{-5}	3.47

function of 0.51 and a weighted rectangle function of 0.49. The final disc surface regression equation adjusted quadratic equation represents roughly 98 percent of the data; Table 6 has the coefficient values.

Obtaining an Equation (11) that illustrates convective heat transfer from the friction surfaces of disc brakes was the subject of the preceding sections. However, four terms in the equation indicate the relative complexity of behavior. Several elements that influence the h_{conv} value

must be simplified to create the relationship. It was claimed, for example, that the surface's relative position was not taken into account. The flow over the surface is affected by the hat part's presence on the outboard side. For example, the air passing through the top rectangle would be hotter than the air passing through the bottom rectangle, which was a final consequence that was overlooked. The heat transfer values in the rectangles at the top and bottom were calculated using identical figures.

On the other hand, this method substantially improves the current temperature estimate for disc brakes in parked conditions. In addition, the convective heat transfer capabilities of a general disc shape geometry oriented vertically in free air have been examined thus far. As a result, this method can now be used to acquire the hat section's h_{conv} value.

5. 3. Convective Heat Transfer Over Hat Section

In the CV brake disc convection research, an identical dimensionless number inquiry was performed on the hat part as it was on the disc friction surface. The buoyant air flow around cylindrical structures has also gotten much attention. For example, a CV brake disc's cylinder-shaped hat section has a high length and diameter; this allows for a lot of heat escape through convection. A pattern in Nusselt numbers for cylinders was observed by Churchill and Chu [12], similar to vertically placed flat walls in free air. For flow across cylindrical bodies, only isothermal surfaces with Rayleigh numbers in the 104 to 1012 range can use their correlation Equation (13).

$$Nu^{1/2} = 0.6 + \frac{0.387 Ra_D^{1/6}}{[1+(0.6/Pr)^{9/16}]^{8/27}} \tag{13}$$

Morgan [11] also proposed a vertical wall correlation Equation (14), which is comparable to the McAdams [10] equation. However, the coefficient values matching flows across a circular surface to the relevant Ra value range.

$$Nu = \frac{h_{conv}D}{k} = cRa_D^n \tag{14}$$

As a result, the dimensionless numbers should all have the same profile, with the scale shifting as the duration of the characteristic varies in Table 7.

TABLE 7. Morgan [11] Equation (14), the Ra_D range values

Ra_D	c	n
10^{10} to 10^2	0.68	0.06
10^2 to 10^3	1.025	0.15
10^3 to 10^4	0.851	0.19
10^4 to 10^7	0.482	0.252
10^7 to 10^{12}	0.128	0.33

By averaging the findings, h_{conv} Equation was constructed. Because it fits Equation (11), the equation format was kept consistent; Table 8 presents the coefficients.

For emissivity calculations, the temperatures range from 0°C to 350°C and 200°C to 1000°C. Given that the temperature range under investigation in this project varies from 20° to 400° C, the cooling test had to be repeated twice to capture data over the entire cooling phase and to ensure consistent values were obtained.

Figure 12 depicts the emissivity result; Emissivity varies with temperature because a body's ability to accept electromagnetic waves decreases as it heats up. Figure 12 shows this pattern, but the decrease in temperature is so minor that the difference in the calculation is negligible. As a result, the emissivity of the grey cast iron disc brake can be assumed constant throughout the stationary parking application.

Previous studies concentrated on determining the thermal distortion and stress levels of a brake rotor [29], reducing the vonmises stresses and displacement vector sum and mass of the brake disc [30], increasing the velocity of mass movement through the passage [31], and calculating deformation and temperature [32].

According to Newcomb [33], Newcomb and Millner [34] the cooling rates of automobile drum and disc brakes. The drums or disc brakes were heated to maintain a consistent temperature using drag braking, and they were timed to see how quickly they cooled while the vehicle was moving at a constant speed. The shape and scale of the disc or drum have been shown to influence cooling rates. Front brake cooling rates are

TABLE 8. HTC coefficients for the hat area in relation to Equation (11)

a_1	a_2	a_3	a_4
-7.37	-0.0100	1.22×10^{-5}	3.13

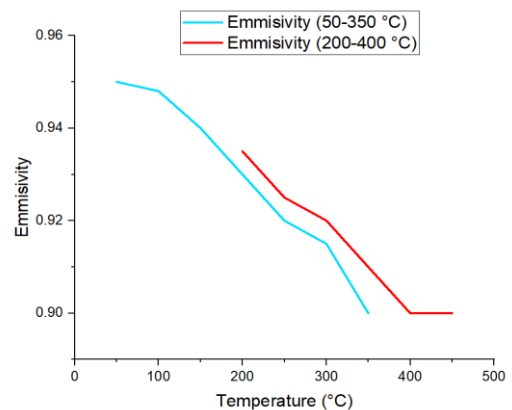


Figure 12. Entire cooling phase, emissivity results

approximately 18% higher than rear brake cooling rates, and front discs cool approximately 22% faster than the optimum drum size for the same car, according to the results. The cooling rate of the front discs did not change when wire wheels were used instead of solid wheels. There was also a comparison of solid and vented discs. Dust shields on disc brakes have been found to reduce cooling rates by approximately 20%. The effect of disrupting airflow in other ways was investigated.

6. VALIDATION

In this section, analytically predicted temperature has been compared to computed values. A comparison of the three numerical analysis results to CFD data is shown in Figure 13, with error bars of 5% added to show the necessary degree of accuracy.

Cases 2 and 3 anticipated temperature profiles are highly similar to case 1, and the temperature is definitely over-predicted by more than the acceptable margin. After the hour mark, the main difference between cases 2 and 3 becomes apparent. When the two profiles parted ways when the disc brake temperature dropped below 125°C in case 2. Using a constant h_{conv} resulted in a slower change in the temperature profile gradient than in case 3. Both approaches are accurate to within a 5 percent margin of error. However, because of the flexibility of convection, case 3 more closely resembles the cooling profile than case 2. It may be determined that a variable coefficient of convection is required to maintain the cooling profile's surface temperature integrity during a temperature change from higher to lower.

Since only a tiny amount of energy may be emitted at temperatures close to ambient, at low temperatures, the increase in h_{conv} can be due to radiation variation. In the previous example, keeping radiation constant resulted in underestimating convection and overestimating emitted

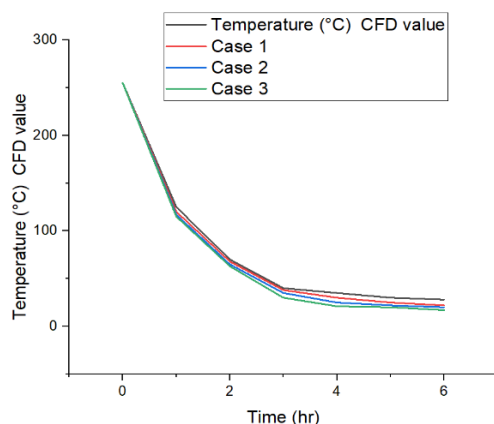


Figure 13. Comparison of the expected (Cases 1, 2 and 3) and measured temperatures CFD value

radiation energy. As a result, the variation in radiative heat transfer as a function of temperature must be taken into account because it was included in the cooling 1st order differential equation, and the numerical results were improved.

7. CONCLUSIONS

In the automotive industry, the research provided has two uses: Commercial vehicle EPB development which is both resilient and accurate, allowing temperature predictions, and EPB management on real-world automobiles. Following interferences can be reported.

- Estimating disc temperatures during the cooling process at 400°C, the value of Ra as 3.5×10^8 indicates a turbulent flow.
- A Nusselt number pattern that appears identical over the arc surface produces 13.38 percent better performance. Nu values at maximum temperature were calculated to be 80.5 and 82.6 at 251.8 °C, respectively.
- When examining a single point along the horizontal center line, the size of the Grashof number increases as temperature falls, peaking at 255.6°C. The kinematic viscosity affects thermal gradient and a temperature of 255.6°C or higher, lowering the Gr value.
- The h_{conv} value was 4.1 percent lower than the arc zone, with a maximum of 11.5 W/m² K at 400°C.

Research limitations/ implications - Correct answers for complex processes such as heat transport and particle tumbling have been achieved using CFD software.

Social implications - The event of automated driving offers a number of possible benefits both on an individual level as well as to the society, such as improved safety and fuel economy, increased heat dissipation and reduced problems with congestions etc.

Findings - It is evident from the findings that convective heat transfer coefficient in all regions improves the disc brake thermal stability.

The expected and measured disc temperatures were relatively close, falling below the 5% tolerance for error. According to numerical solutions produced in heat transfer, coefficients and temperatures were averaged over the main disc surfaces to grasp a CV brake disc heat dissipation better. CFD modeling has helped to evaluate flow patterns and h_{conv} fluctuation throughout the entire disc brake surface area. In addition, the investigation has helped to assess appropriate modeling methodologies for calculating heat transfer coefficients for all disc regions.

The CFD software have been used so that correct solutions for complex processes, such as heat transmission and particle tumbling, may be achieved.

Regarding the outlook, there are three recommendations for the expansion of future work

related to disc brake that can be done to further understand the effects of the thermal stability of the disc brake, the recommendations are as follows:

1. Experimental study to verify the accuracy of the numerical model developed.
2. Tribological and vibratory study of the contact disc – pads;
3. Study of dry contact sliding under the macroscopic aspect (macroscopic state of the surfaces of the disc and pads).

8. REFERENCES

1. Slosarczyk, K., Linden, J., Burnham, K., Cockings, K. and Capolongo, R., "Implementation of an electronic park brake feature with limited data availability", in 2008 19th International Conference on Systems Engineering, IEEE., (2008), 254-259.
2. Peng, Y.-q. and Li, W., "Research on fuzzy control strategies for automotive epb system with amesim/simulink co-simulation", in 2009 Chinese Control and Decision Conference, IEEE., (2009), 1707-1712.
3. Lee, C., Chung, H., Lee, Y., Chung, C., Son, Y. and Yoon, P., "Fault detection method for electric parking brake (epb) systems with sensorless estimation using current ripples", *International Journal of Automotive Technology*, Vol. 11, No. 3, (2010), 387-394.
4. Galindo-Lopez, C. and Tirovic, M., "Understanding and improving the convective cooling of brake discs with radial vanes", *Proceedings of the Institution of Mechanical Engineers, Part D: Journal of Automobile Engineering*, Vol. 222, No. 7, (2008), 1211-1229.
5. Voller, G., Tirovic, M., Morris, R. and Gibbens, P., "Analysis of automotive disc brake cooling characteristics", *Proceedings of the Institution of Mechanical Engineers, Part D: Journal of Automobile Engineering*, Vol. 217, No. 8, (2003), 657-666.
6. McPhee, A.D. and Johnson, D.A., "Experimental heat transfer and flow analysis of a vented brake rotor", *International Journal of Thermal Sciences*, Vol. 47, No. 4, (2008), 458-467.
7. Liang, L., Jian, S. and Xuele, Q., *Study on vehicle braking transient thermal field based on fast finite element method simulation*. 2005, SAE Technical Paper.
8. Bagnoli, F., Dolce, F. and Bernabei, M., "Thermal fatigue cracks of fire fighting vehicles gray iron brake discs", *Engineering Failure Analysis*, Vol. 16, No. 1, (2009), 152-163.
9. Tirovic, M. and Voller, G., "Interface pressure distributions and thermal contact resistance of a bolted joint", *Proceedings of the Royal Society A: Mathematical, Physical and Engineering Sciences*, Vol. 461, No. 2060, (2005), 2339-2354. doi.
10. McAdams, W., "Heat transfer", *McGraw-Hill, New York*, Vol. 1, No. 51, (1954), 3.
11. Morgan, V.T., The overall convective heat transfer from smooth circular cylinders, in *Advances in heat transfer*. 1975, Elsevier.199-264.
12. Churchill, S.W. and Chu, H.H., "Correlating equations for laminar and turbulent free convection from a horizontal cylinder", *International journal of heat and mass transfer*, Vol. 18, No. 9, (1975), 1049-1053.
13. Ozisik, M.N., "Heat transfer: A basic approach, McGraw-Hill New York, Vol. 780, (1985).
14. Richardson, P. and Saunders, O., "Studies of flow and heat transfer associated with a rotating disc", *Journal of Mechanical Engineering Science*, Vol. 5, No. 4, (1963), 336-342.
15. Fletcher, L., "Recent developments in contact conductance heat transfer", (1988).
16. Bergman, T.L., Lavine, A.S., Incropera, F.P. and DeWitt, D.P., "Introduction to heat transfer, John Wiley & Sons, (2011).
17. Moffat, R.J., "Describing the uncertainties in experimental results", *Experimental Thermal and Fluid Science*, Vol. 1, No. 1, (1988), 3-17.
18. Moffat, R.J., "Using uncertainty analysis in the planning of an experiment", (1985).
19. Nakos, J.T., *Uncertainty analysis of thermocouple measurements used in normal and abnormal thermal environment experiments at sandia's radiant heat facility and lurance canyon burn site*. 2004, Sandia National Laboratories (SNL), Albuquerque, NM, and Livermore, CA
20. Taylor, J., "Introduction to error analysis, the study of uncertainties in physical measurements, (1997).
21. Taylor, J.R., *University science books*. 1982, Mill Valley California.
22. Stevens, K. and Tirovic, M., "Heat dissipation from a stationary brake disc, part 1: Analytical modelling and experimental investigations", *Proceedings of the Institution of Mechanical Engineers, Part C: Journal of Mechanical Engineering Science*, Vol. 232, No. 9, (2018), 1707-1733.
23. Stevens, K., Leiter, R. and Taylor, M., "Thermal aspects in electronic parking braking of commercial vehicles", in European conference on braking., (2010).
24. Noroozi, M.J., "Investigation of the effects of non-linear and non-homogeneous non-fourier heat conduction equations on temperature distribution in a semi-infinite body", *International Journal of Engineering, Transactions C: Aspects*, Vol. 28, No. 12, (2015), 1802-1807. doi: 10.5829/idosi.ije.2015.28.12c.14.
25. Goudarzi, K., Shojaefard, M. and Fazelpour, M., "Effect of contact pressure and frequency on contact heat transfer between exhaust valve and its seat", *International Journal of Engineering, Transactions B: Applications* Vol. 21, No. 4, (2008), 401-408.
26. Viviani, A. and Pezzella, G., "Heat transfer analysis for a winged reentry flight test bed", *International Journal of Engineering*, Vol. 3, No. 3, (2009), 329-345.
27. Kostikov, Y.A. and Romanenkov, A.M., "Approximation of the multidimensional optimal control problem for the heat equation (applicable to computational fluid dynamics (CFD))", *Civil Engineering Journal*. Vol. 6, No. 4, (2020), 743-768. doi: 10.28991/cej-2020-03091506.
28. Abderrahmane, B., Naima, B., Tarek, M. and Abdelghani, M., "Influence of highway traffic on contamination of roadside soil with heavy metals", *Civil Engineering Journal*, Vol. 7, No. 8, (2021), 1459-1471. doi: 10.28991/cej-2021-03091736.
29. Valvano, T. and Lee, K., "An analytical method to predict thermal distortion of a brake rotor", *SAE Transactions*, (2000), 566-571.
30. Kumar, G.R., Thriveni, S., Reddy, M.R. and Gowd, G.H., "Design analysis & optimization of an automotive disc brake", *International Journal of Advanced Engineering Research and Science*, Vol. 1, No. 3, (2014), 24-29.
31. More, A.V. and Sivakumar, R., "Cfd analysis of automotive ventilated disc brake rotor", *Int. Journal of Engineering Research and Applications, ISSN*, Vol., No. 2248-9622.
32. Jaligama, S.K., Choudhary, P., Kumar, K.C., Prashanth, B. and Sreekanth, D., "Cfd and thermal analysis of atv disc brake", *International Journal of Research and Technology*, Vol. 7, (2020), 1511-1516.

33. Newcomb, T., "Transient temperatures in brake drums and linings", *Proceedings of the Institution of Mechanical Engineers: Automobile Division*, Vol. 12, No. 1, (1958), 227-244.
34. Newcomb, T. and Millner, N., "Cooling rates of brake drums and discs", *Proceedings of the Institution of Mechanical Engineers: Automobile Division*, Vol. 180, No. 1, (1965), 191-205.

Persian Abstract

چکیده

هدف مطالعه حاضر توسعه ترمز دستی الکتریکی (EPB) برای وسایل نقلیه تجاری (CVs) است. رزومه‌هایی با برنامه‌های EPB در حال حاضر در مجموعه‌ای کاملاً متفاوت از برنامه‌های EPB در خودروهای سواری که در حال حاضر به طور گسترده استفاده می‌شوند، در دسترس هستند. پارک ایمن نیاز به تمرکز بسیار بیشتری با مرتبه بزرگی، ظرفیت حرارتی بیشتر، جرم ترمز و فشار گیره دارد. در مرحله اول، تلفات حرارتی از دیسک ترمز برآورد شد. بررسی‌ها همچنین امکان پیش‌بینی دقیق اتلاف حرارت تشعشعی را با تعریف گسیل سطحی فراهم کردند. پارامترهای حرکت هوا، ضرایب انتقال حرارت همرفتی و سرعت مورد بررسی قرار گرفت و اعتبارسنجی با مدل CFD انجام شد. هنگامی که دما به ۲۵۲ درجه سانتیگراد کاهش یافت، حداکثر مقدار تخمینی عدد ناسلت ۷۲/۲۵ بود. الگوی عدد ناسلت که روی سطح قوس یکسان به نظر می‌رسد، ۱۳/۳۸ درصد نتایج بهتری به همراه دارد. مقادیر Nu در حداکثر دما ۸۰/۵ و ۸۲/۶ در ۲۵۱/۸ درجه سانتیگراد محاسبه شد. مقدار " h_{conv} " ۴/۱ درصد کمتر از ناحیه قوس بود، با بالاترین مقدار در ۴۰۰ درجه سانتیگراد ۱۱.۵ $W/m^2 \cdot K$. مطالعه حاضر رویکرد منحصر به فردی را اتخاذ کرد و دمای دیسک ترمز و ضریب انتقال حرارت همرفتی را روی سطوح اصطکاک دیسک و مناطق کلاه به دست آورد. مدل سازی CFD در طول فاز خنک کننده برای ارزیابی الگوهای جریان و نوسانات " h_{conv} " در کل سطح ترمز دیسکی انجام شد. مدل سازی ریاضی و روش اتخاذ شده برای محاسبه ضرایب انتقال حرارت برای مناطق مختلف دیسک به درک بهتر اتلاف حرارت دیسک ترمز CV کمک کرده است.
